VALIDATION REPORT
DLST (LSA-003A & LSA-003B)

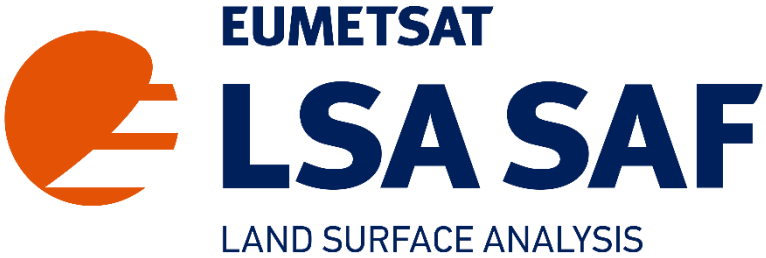

Reference Number:	SAF/LAND/KIT/VR_DLST/1.0
Issue/Revision Index:	Issue 2
Last Change:	29/07/2016

DOCUMENT SIGNATURE TABLE

	Name	Date	Signature
Prepared by :	F. Göttsche		
Approved by :	LSA SAF Project Manager (IPMA)		

DOCUMENTATION CHANGE RECORD

Issue / Revision	Date	Description:
Version 1.0 Issue 2	07/10/2015 28/07/2016	Version to be presented to ORR Revised following Reviewers' suggestions.

Executive Summary

Land Surface Temperature (LST) retrieved from MSG/SEVIRI data (MLST; LSA-001) is generated on an operational basis since February 2005 for the European region and since July 2005 for the whole Meteosat disk. For completely cloud-free days the 96 daily MLST per pixel resolve the diurnal temperature cycle (DTC) of the land surface at SEVIRI's full temporal resolution (15 min). However, generally clouds reduce the number of available MLST considerably. Forming maximum composites per observation time-slot within a 10-day period is a well-established and simple method to obtain spatially more continuous maps (Holben, 1986).

When treating the sequence of composited LST obtained for each SEVIRI time slot as a 'synthetic DTC', these can be analysed with the same methods as for cloud-free days. The Derived Land Surface Temperature (DLST) product (LSA-003) provides a 10-day synthesis of the LSA SAF MLST product (LSA-001). This is achieved in two steps: (i) maximum and median LST within the compositing period and per time-slot are formed, leading to a maximum and median value every 15 minutes (LSA-003A); (ii) a DTC model is fitted to the sequence of LST composites to obtain the Thermal Surface Parameters (TSP). Here, the model of Göttsche and Olesen (2009) is used to obtain the TSP, which then summarize the synthetic DTC described by the sequence of MLST composites (LSA-003A). The TSP are disseminated as LSA-003B product and present an effective compression of the 15 minute information (up to 96 values per DTC), through a small number (7) of easy to interpret parameters. Furthermore, the modelling reduces data gaps and noise (e.g. from cloud contamination) that may still be contained in the composites. MLST composites (LSA-003A) and TSP (LSA-003B) are both part of the DLST product. The LSA-SAF product MLST (LSA-001) and the composite product COMDLST (LSA-003A) are closely related to each other, so that the validation results presented in the 'LandSAF VR-LST' also apply to COMDLST. Here, we exclusively present the validation results obtained for the LSA-SAF DLST product LSA-003A (maximum and median composites) and LSA-003B (TSPDLST).

The DLST median and maximum compositing algorithms (LSA-003A) were successfully tested using various combinations of synthetic LST input fields. Satellite-derived LST composites were compared with composites of in-situ LST from validation station Gobabeb, Namibia. The resulting differences in composite LST were within the expected range.

The DTC model of Göttsche and Olesen (2009) was shown to correctly reproduce the slow and smooth increase of LST around sunrise and it has the ability to temporally "squash" modelled DTC to match the shape of the actual DTC. A Levenberg-Marquardt minimisation scheme was used to fit the model to 54 DTC from a validation site in an arid climate (Gobabeb, Namibia) and to 100 DTC from a site in temperate climate (Evora, Portugal). The results demonstrate the high accuracy achieved by the DTC model and its ability to reproduce the general shape of cloud-free DTC: the average of daily mean absolute deviation between modelled and measured DTC is 0.62 °C for Gobabeb and 0.97 °C for Evora, where the latter is thought to be the result of cloud-contamination.

Operational TSP (LSA-003B) are obtained from decadal MLST composites (LSA-003A). For an area with a sufficient number of cloud-free MLST (LSA-001), the mean absolute deviation between median LST composites and modelled DTC was 0.73 K ±0.33 K, i.e. about half the MLST product's target accuracy. From these results it is concluded that the Göttsche and Olesen (2009) model describes the DTC as given by sequences of MLST (LSA-001) and their temporal composites (DLST; LSA-003A) well.

TABLE OF CONTENTS

List of Tables

List of Figures

1 Introduction

Satellite based remote sensing is the only realistic means by which the land surface can be monitored frequently and on large scales. The last decades have seen a steady increase of space-borne sensors with ever increasing capabilities with respect to spectral, spatial, and temporal resolution, e.g. compared to its predecessor the data volume produced by MSG/SEVIRI has risen from 1 Terabyte to 20 Terabyte per year. The trend to ever larger data volumes is set to continue and will require more automated data processing and algorithms capable of extracting and summarizing the relevant information. Further challenges are posed by analyses of relations between independent space-derived parameters, e.g. LST and vegetation indices, which have to be systematically studied and interpreted in the framework of global change research (Stoll, 1994; Lambin and Ehrlich, 1996).

The EUMETSAT Satellite Application Facility on Land Surface Analysis (LSA SAF) generates, on an operational basis, Land Surface Temperature (LST) for SEVIRI on-board the MSG satellites (Schmetz et al., 2002a). The LSA SAF LST product for MSG (MLST; LSA-001) is processed at the full SEVIRI temporal and spatial resolution and captures the diurnal LST cycle over clear sky regions. The high sampling rate of MSG/SEVIRI (15 min) allows to accurately determine the time and value of the daily maximum LST as well as to create 'synthetic' diurnal temperature cycles (DTC), which then can be analysed with methods developed for individual (cloud-free) DTC. However, even though maps of decadal LST composites are spatially more continuous than individual LST maps, they can still be affected by persistent cloud-cover and undetected clouds, which results in missing or noisy data. Göttsche and Olesen (2001) fitted a simple physics-based model to (cloud-free) DTC to summarize the thermal behaviour of the land surface; the modelling yields sets of representative and informative "Thermal Surface Parameters (TSP)", which can be used to reconstruct complete DTCs, to interpolate atmospheric corrections and missing LST (Schädlich et al., 2001; Jiang et al., 2006; Inamdar et al., 2008, Inamdar and French, 2009) and for improving cloud screening algorithms (Reuter, 2005; Stöckli, 2013). In the LSA SAF LSA-003B product the TSP are obtained by fitting an improved DTC model (Göttsche and Olesen, 2009) to synthetic diurnal cycles described by temporal composites of MLST. The MLST composites (LSA-003A) approximate cloud-free DTC and are summarized by the corresponding TSP (LSA-003B). The DLST product (LSA-003) consist of the MLST composites and the TSP.

This report presents validation results obtained for the LSA SAF product LSA-003A (maximum and median composites of MLST product) and LSA-003B (i.e. the TSP). The validation is based on in-situ data from KIT's permanent LST validation stations in Europe and Africa and on median and maximum MLST composites (COMDLST; LSA-003A). Details on the DLST (LSA-003) product and its performance are given in the 'Algorithm Theoretical Basis Document (ATBD) for DLST' (Göttsche, 2014), the 'Product User Manual (PUM) Land Surface Temperature' (Land SAF Project Team, 2017), and the 'SAF for Land Surface Analysis (LSA SAF) Validation Report LST' (Trigo et al., 2015).

The LSA-003A and LSA-003B products are derived from LSA SAF 15-min LST product estimated from SEVIRI/Meteosat (LSA-001) and, therefore, their accuracy depends essentially on that of LSA-001 and on the correctness of the compositing algorithms applied. The LSA-001 product has been extensively validated against in situ stations and was shown to meet the product requirements (Ermida et al., 2014; Göttsche et al., 2016), which coincide with those established for LSA-003 (Table 1). Here we assess both, the algorithm that generates LSA-003 and the product. The algorithm and product verification indicates that LSA-003A and LSA-003B meet the accuracy requirements (Table 1).

Table 1 Accuracy Requirements for LSA-003 product (applicable to both LSA-003A and LSA-003B). The same accuracy requirements have been set for LSA SAF 15-min LST product (LSA-001), which is the base for LSA-003.

Threshold Accuracy	Target Accuracy	Optimal Accuracy
4 K	2K	1K

2 Derived Land Surface Temperature Products

2.1 Median and Maximum LST Composite – LSA-003A

The median and maximum LST composite products (LSA-003A) are based on the LSA-SAF operational LST product LSA-001; therefore, they share most of LST_SEVIRI's characteristics, e.g. in terms of accuracy and spatial resolution. LSA-003A products are produced on a decadal basis (every 10 days) for each MSG/SEVIRI slot (15 min) and approximate cloud-free LST at the time of the slot.

2.2 Diurnal temperature cycle (DTC) models – LSA-003B

The DTC models of Göttsche and Olesen (2001) and Göttsche and Olesen (2009) are described in some detail in the 'LSA SAF ATBD for DLST' (Göttsche, 2014). In the following, only the implemented 'Goe2009' model will be discussed. Duan et al. (2012) found that the Goe2009 model performed favourably compared to other DTC models. The various model parameters, the so-called 'Thermal Surface Parameters (TSP)', are listed in Table 2 and illustrated in Figure 1: the LSA SAF DLST product LSA-003B is obtained using the Goe2009 model (solid line).

Table 2 Meaning of the model parameters (see Figure 1).

Parameter		Meaning
T_o	[°C]	minimum temperature
T_a	[°C]	temperature amplitude $(=T_{max}-T_0)$
t_m	[solar time]	time of the maximum
t_s	[solar time]	start of the attenuation function
δT	[°C]	$T_o - T(t\rightarrow\infty)$, where t is time
k	[hh:mm]	attenuation constant (via continuity condition)
τ		total optical thickness (TOT)

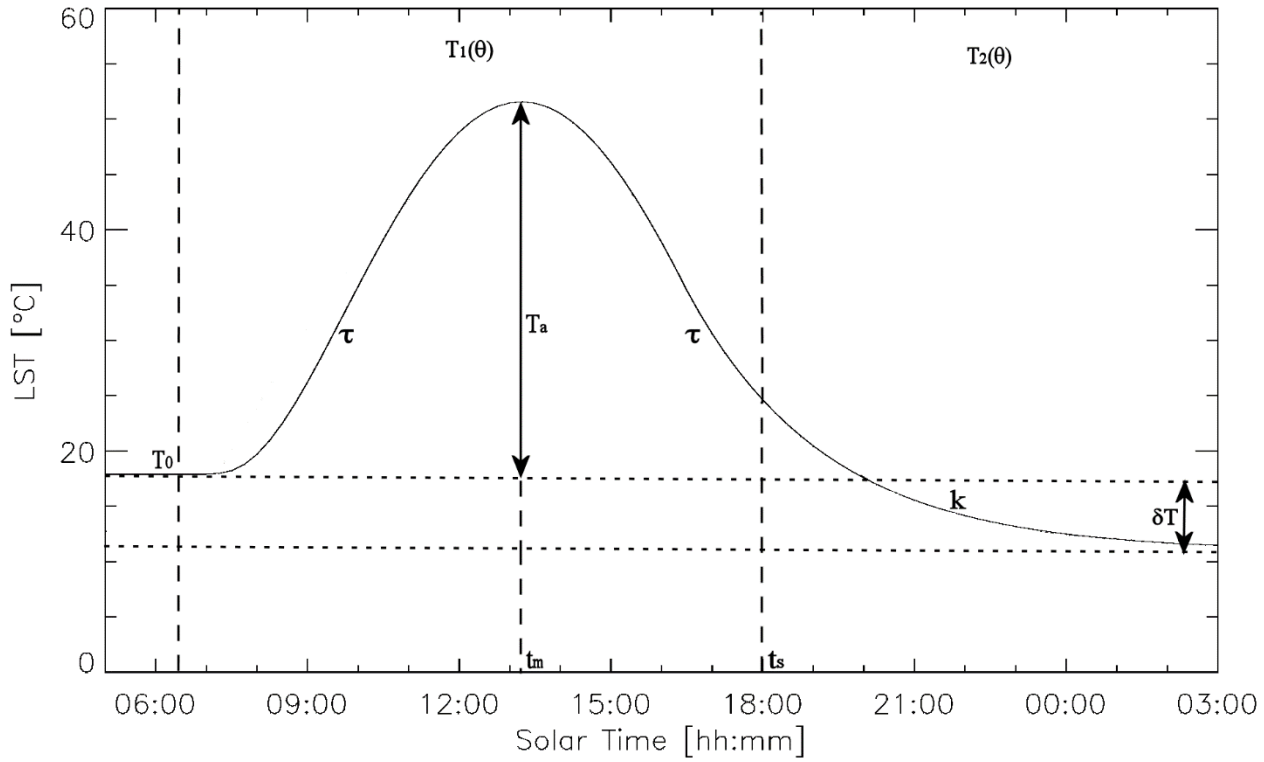

Figure 1 Model parameters (Table 2) and fits of the DTC model "Goe2009" (solid line) developed by Göttsche and Olesen (2009) to sample LST (data omitted for clarity). The "daytime" part T1 (sunrise to start of attenuation function at ts) and the "night-time" part T2 (ts to end, here 03:00h) of the model is indicated by broken vertical lines.

3 LST validation stations

In order to be able to validate satellite-derived LST products over a wide range of surface and climatic conditions, Karlsruhe Institute of Technology (KIT) set up four permanent LST validation stations in areas characterised by naturally homogeneous land use and land cover in different climate zones. The stations are part of LSA-SAF's validation effort and were chosen and designed to validate LST derived from MSG/SEVIRI, but are equally well suited to validate LST products from other sensors. Figure 2 shows the stations' locations within the field of view (FOV) of the METEOSAT satellites: Evora (Portugal, since 2005; cork-oak trees and grass), Dahra (Senegal, since 2008; tiger bush), Gobabeb (Namibia, since 2007; gravel plain), and RMZ farm / farm Heimat (Namibia, since 2009; Kalahari bush). Station Evora is in temperate Mediterranean climate (CSh), Dahra in semi-arid climate (BSh), and Gobabeb & Kalahari are in warm desert climate (BWh) climate zones, respectively (Köppen, 1936).

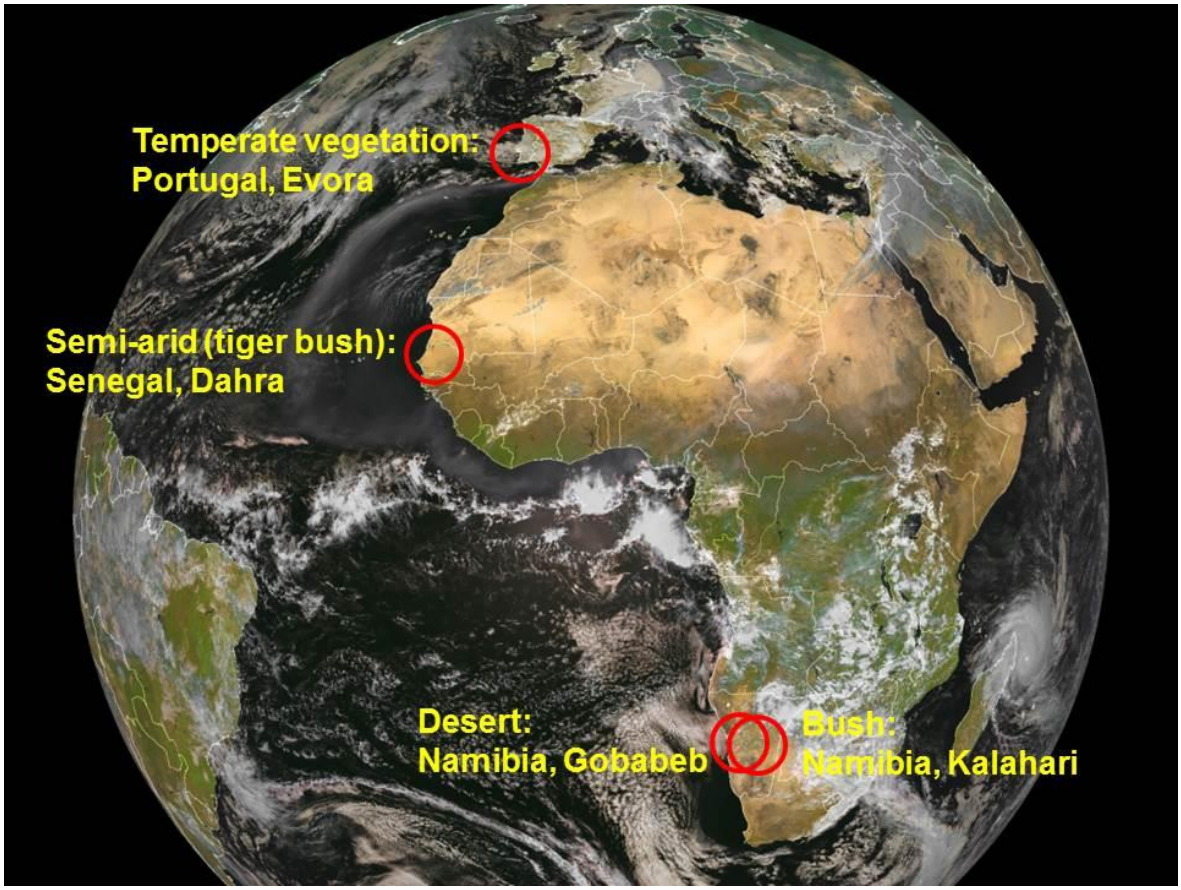

Figure 2 Locations of KIT's validation stations on MSG/SEVIRI earth disk.

The LSA-001 product, which is the main input for LSA-003, has been extensively validated against the stations shown in Figure 2; the respective results are detailed in Ermida et al. (2014) and Göttsche et al. (2016), as well as in the LSA-001 product Validation Report (please see most recent version of SAF_LAND_VR_LST available from the LSA SAF site). The validation performed for LSA-001 over recent years shows that that product meets the requirements indicated in Table 1. The LSA-003A product has been validated by performing numerical tests on the algorithms and by verifying the respective product values against maximum and median composites of in situ LST observations at KIT stations (Figure 2).

In order to validate the Goe2009 model, which is used to obtain the LSA-003B product, Göttsche and Olesen (2009) fitted the model to LST time series of 54 days and 100 days for Gobabeb and Evora validation sites, respectively. The time series are from periods with low cloud frequency and no additional cloud-masking was performed.

4 Validation Results

4.1 Validation of LSA-003A

4.1.1 Composite Algorithm Validation for synthetic input data

The compositing algorithm was first checked for consistency using a set of synthetic input fields generated as in the same format as HDF-5 MLST (LSA-001) files. This allows verifying that maximum and median LST values are also correctly estimated for combinations of extreme LST observations, e.g. with and without missing values or for an even and odd number of records. The algorithms consistency was checked by setting complete LST input fields to easily recognised values.

First, ten LST fields for the "SAfr" subset were set to: 0.0, 5.0, 10.0, 15.0, 20.0, 25.0, 30.0, 35.0, 40.0, and 45.0 °C. For each pixel the correctly determined median was 22.5 °C and the maximum 45.0 °C. Then the algorithm performance for **odd** numbers of input LST fields was checked by setting nine LST input fields to 0, 5.0, 10.0, 15.0, 20.0, 25.0, 30.0, 35.0, and 40.0 °C: the correctly determined values for each pixel were 20.0 °C and 40.0 °C for the median and maximum, respectively. In order to check correct performance when including negative LST values, composites were obtained for ten LST fields set to -20.0, -15.0, -10.0, -5.0, 0.0, 5.0, 10.0, 15.0, 20.0, and 25.0 °C. For each pixel the determined median was 2.5 °C and the maximum 25.0 °C. Finally, for nine LST fields set to -20.0, -15.0, -10.0, -5.0, 0.0, 5.0, 10.0, 15.0, and 20.0 °C, for each pixel the median was 0.0 °C and the maximum was 20.0 °C. For all tested combinations of synthetic LST fields the respective composites over the entire SAfr subset were determined correctly.

4.1.2 Product Validation

Figure 3 and Figure 4 show the median and maximum composite at 13:00 UTC for the decade from the 01.06. to the 10.06.2011 for LSA-SAF's "Southern Africa (SAfr)" subset. No additional cloud-filtering is applied in the determination of LST composites. At this time it is winter in the southern hemisphere, which shows particularly in the low temperatures around the Cape of Good Hope. Both composites are spatially continuous and have only few missing data near the equator, i.e. over the Tropics where clouding is usually very persistent. Generally, the median composite is more detailed than the maximum composite, i.e. its spatial structures are finer. High temperatures are observed in considerably larger parts of the maximum composite, e.g. the "band" of the high LST between 15°S and 20°S is wider and the red "strip" along the West coast stretches further to the South (Namib desert; see 25°S, 15°E).

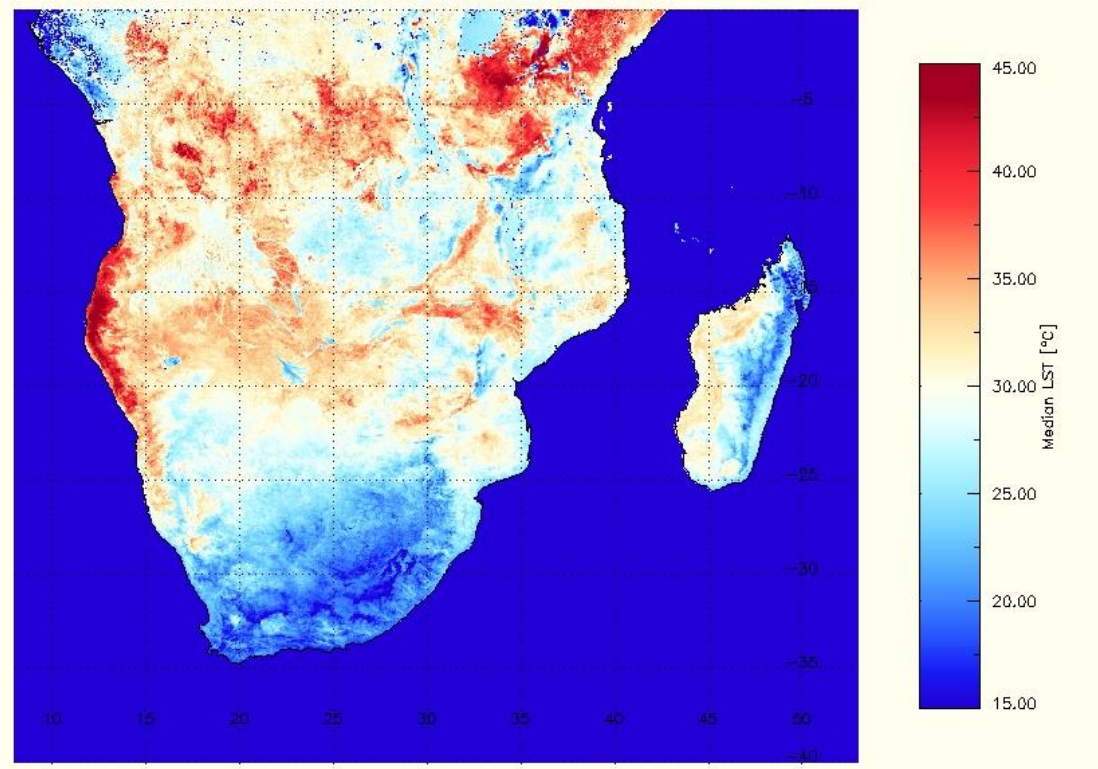

Figure 3 Median composite of the LSA-4 LST product at 13:00 UTC for the decade 01.06. - 10.06.2011.

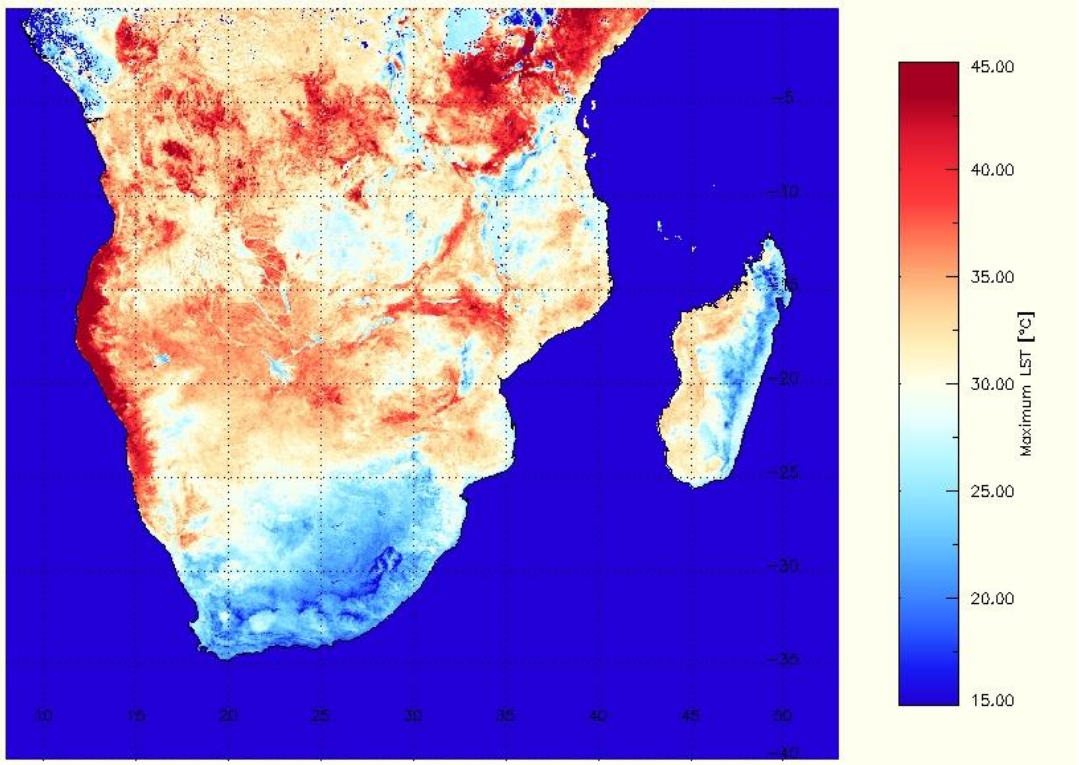

Figure 4 Maximum composite of the LSA-4 LST product at 13:00 UTC for the decade 01.06. - 10.06.2011.

In order to illustrate the typical differences between median and maximum LST composites, Figure 5 shows the histograms for the two composites obtained at 13:30 UTC for the third decade in March 2015 over Eurasia and Africa (MSG/SEVIRI disk shown in Figure 2). The shapes of the two

distributions are similar and - as to be expected - the distribution for the maximum LST composite is shifted to higher values.

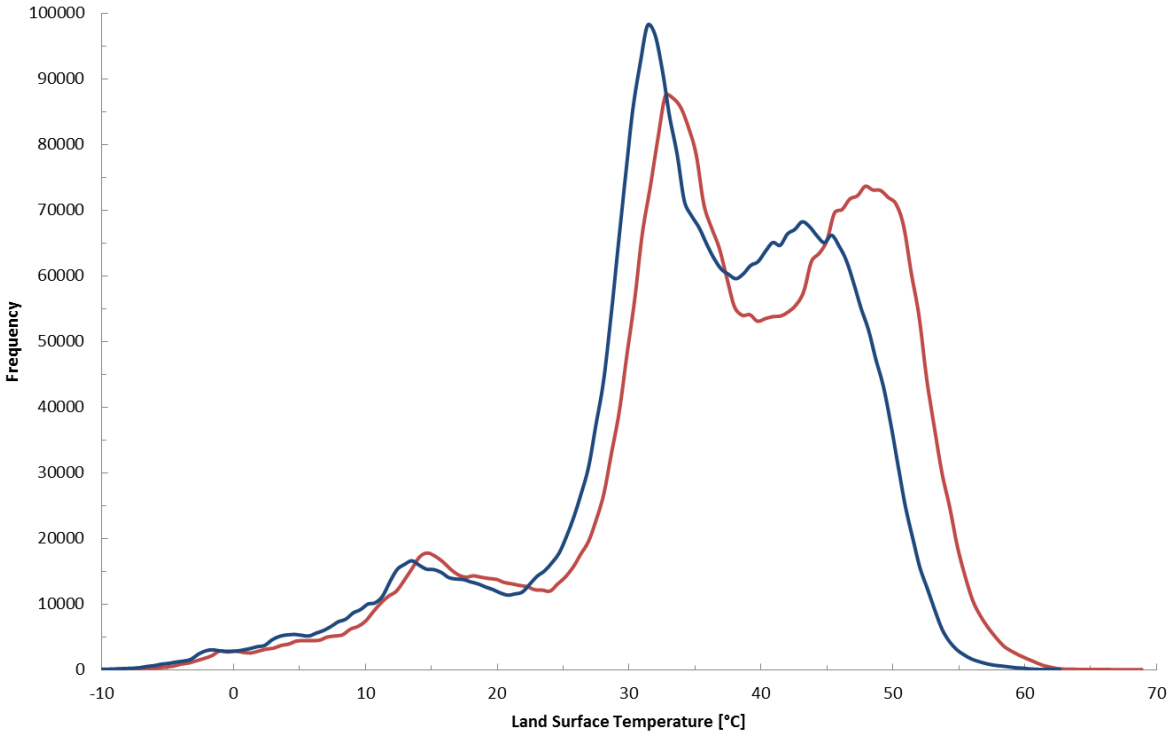

Figure 5 Histograms for median (dark blue) and maximum LST composites (red) obtained at 13:30 UTC for the third decade in March 2015 over Eurasia and Africa.

Figure 6 shows the histogram of the differences between the maximum and median LST composites at 13:30 UTC for the third decade in March 2015. The minimum difference is 0.0°C, i.e. maximum LST are never smaller than the corresponding median LST: therefore, this basic requirement for algorithm consistency is met. The main peak of the distribution is at 1.5°C, i.e. this is the value by which maximum LST exceeds median LST most frequently. The spike at 0.1°C (cut off) represents 'no data' values (mainly sea surface & clouds). However, the difference between maximum and median LST composites varies with geographical region, e.g. over the Sahara the most frequent difference between the two composites (13:30 UTC, third decade in March 2015) is 4.4°C while it is 1.2°C over southern Africa.

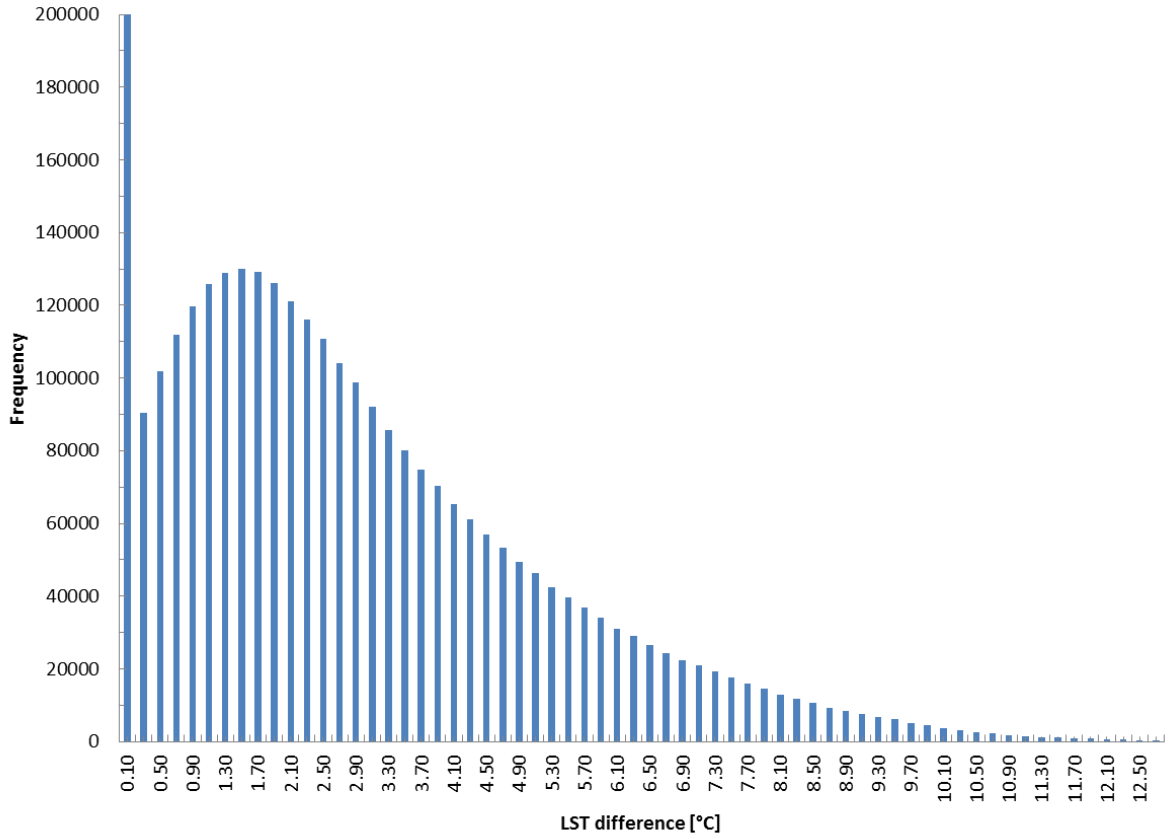

Figure 6 Histogram of (maximum LST - median LST) at 13:30 UTC, third decade in March 2015 for Eurasia and Africa observed by MSG/SEVIRI.

Finally, median and maximum in-situ LST at Gobabeb for the first 10 days in December 2011 were compared against corresponding DLST (LSA-003A) composite values. Six cloud-free observations at 13:00h UTC were available, which had a median of 35.82 °C for the in-situ LST and 34.61°C for the MLST (difference of 1.21°C). The corresponding maximum LST were 40.35°C for the in-situ LST and 39.39°C for the MLST (difference of 0.96°C). However, due to limited number of composited LST values (e.g. 6) and the actual differences between in-situ LST and MLST, the respective median and maximum values are not expected to be identical, particularly when there is some bias between in-situ LST and satellite LST. Therefore, the first 10 days of December 2011 are investigated, for which the MLST have a bias of -0.01 K and a rmse of 1.36 K w.r.t. Gobabeb in-situ LST, which is well within the products target accuracy (Table 1). The median and maximum LST at the four synoptic hours (Table 3) show very good agreement between the respective values obtained for in-situ LST and for MLST composites. The larger difference between the median LST at 06:00 UTC stems from systematically lower in-situ LST at that time; a possible explanation for this would be that the station's proximity to the high dunes of the Namib sand sea causes local differences (wind, fog) around the early morning at this time of the year (Summer on southern hemisphere). However, generally the LST differences are less than LSA SAF's target accuracy (2 K) and also reflect the accuracy typically found for the MLST product (LSA-001; see SAF_LAND_IPMA_VR_LST) over Gobabeb. Therefore, the results support the correct functioning of the compositing algorithms.

Table 3 Median and maximum LST obtained from in-situ data and MLST (LSA-001) for the first 10 days in December 2011 at Gobabeb. For this decade the satellite-retrieved MLST have a particularly small bias (-0.01 K) w.r.t. in-situ LST.

Composite for 1-10 Dec 2011	LST [°C] at 00:00 UTC		LST [°C] at 06:00 UTC		LST [°C] at 12:00 UTC		LST [°C] at 18:00 UTC	
	In-situ	MLST	In-situ	MLST	In-situ	MLST	In-situ	MLST
Median	18.09	18.26	22.42	25.66	57.18	56.89	28.23	28.43
Maximum	21.59	20.77	27.18	27.29	59.47	60.03	29.79	29.9

4.2 Validation of LSA-003B

4.2.1 Algorithm Validation: Fits to individual DTC from Evora, Portugal

Evora LST validation station (38.540° N, 8.003° W, 230m a.s.l.) is located about 12 km south-west of the town of Evora in the Alentejo region, Portugal (Figure 2). The dominant vegetation types at Evora station are isolated groups of evergreen oak trees (quercus ilex, quercus rotundifolia, quercus suber) and grassland, which is mainly used for grazing cattle. The cork oak trees are protected by law and, therefore, have a stable age distribution and a high average age. The climate at Evora station is warm temperate (Peel et al., 2007) with hot, dry summers, annual temperature averages between 15°C and 16°C and an average annual precipitation of 669 mm (Pereira et al., 2007). From about May to September the grass is usually desiccated so that the oak trees are the dominant green vegetation. In contrast, November to March are wet months with a rapidly developing vegetation cover: the combined effect is a strong annual amplitude of green vegetation.

The performance of the model is investigated using diurnal cycles of in-situ LST obtained over a grass surface (emissivity set to 0.98) at Evora station. Modelling results for the in-situ LST are shown in Figure 7 and Figure 8. The mean fit error (measured LST – modelled LST) for 100 days at 15 minutes interval is shown in Figure 7. The mean fit error for Goe2009 (i.e. the model used by the LSA-003B algorithm) reaches only up to -1.8K (around 17 hours). The model has a positive mean error around 16 hours and negative mean error around 17 hours, i.e. on average it first underestimates and then overestimates DTC. However, the mean fit error of the Goe2009 model stays below 2.0°C at any time of the day.

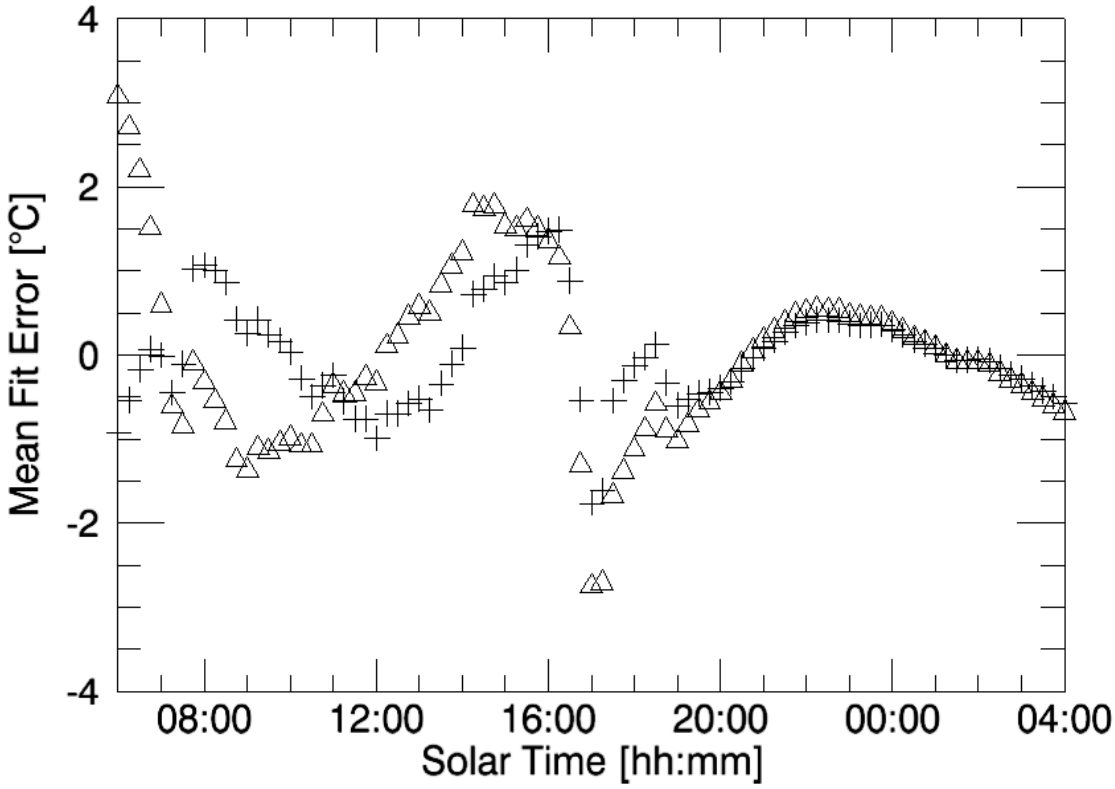

Figure 7 Crosses show the mean error at 15min interval over 100 days between KT-15 LST and Goe2009 LST for at Evora, Portugal (11.06.2008 to 08.11.2008). Triangles show results for a previous version of the DTC model.

Figure 8 shows a histogram of daily mean absolute deviation between measured LST and modelled LST for Goe2009. The histogram represents the same 100 days used in Figure 7. The mean of the histogram is 0.97°C and the distribution appears to be uni-modal with its peak near 0.8°C.

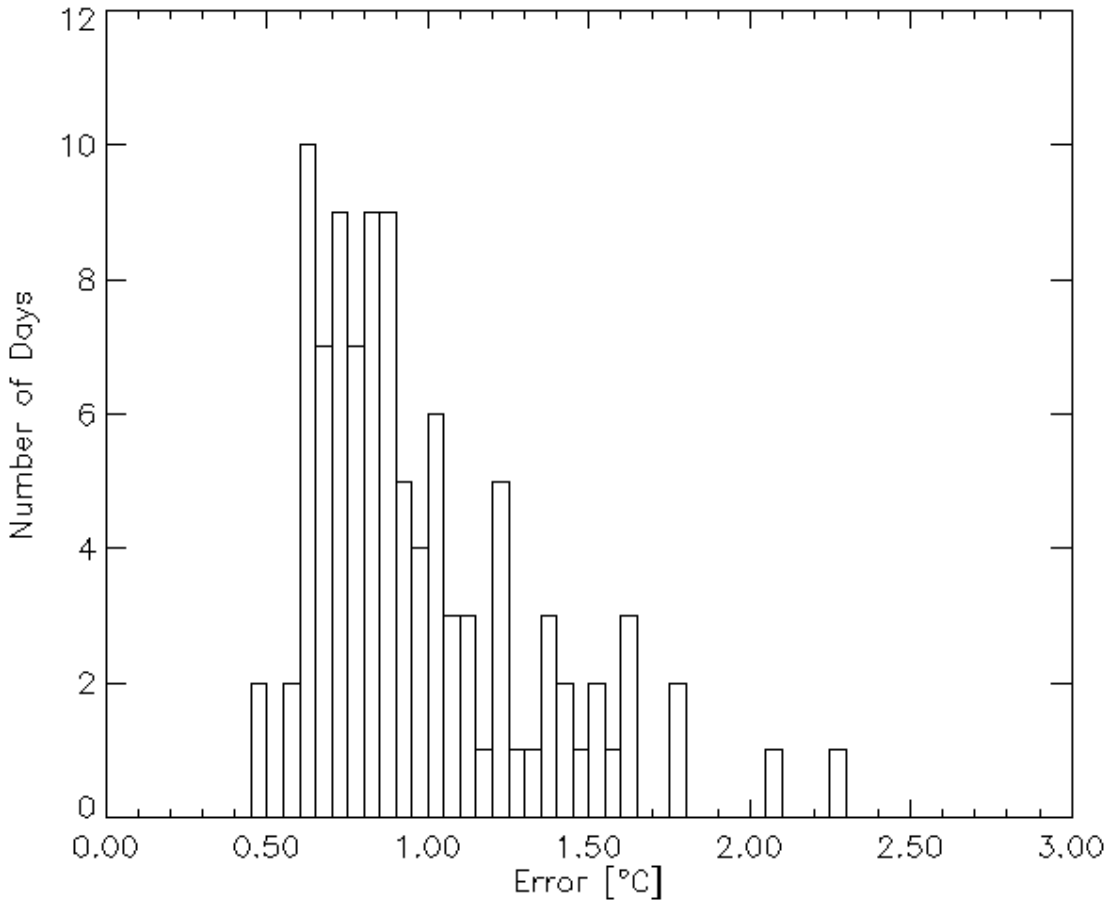

Figure 8 Histogram of mean absolute deviation per day for Goe2009, as used in the LSA-003B product algorithm, fitted to 100 diurnal temperature cycles measured at Evora, Portugal.

4.2.2 Algorithm Validation: Fits to individual DTC from Gobabeb, Namibia

Gobabeb LST validation station (23.551° S, 15.051° E, 450m a.s.l.) lies about 2 km north-east of Gobabeb Training & Research Centre (www.gobabebtrc.org) in the Namib Desert, Namibia (Figure 2). The validation station is located on large gravel plains (several thousand km^2), which are covered by a highly homogeneous mixture of gravel, sand and sparse desiccated grass. There is a sharp transition between the vast Namib sand sea with its up to 300 m high dunes and the gravel plains: this natural boundary is maintained by irregular flows of the ephemeral Kuiseb River (a few days every other year), which wash the advancing sand into the South Atlantic Ocean. Due to the hyper-arid desert climate (Köppen, 1936; Peel et al, 2007), the site is spatially and temporally highly stable and, therefore, ideal for long-term validation studies of satellite products (Hulley et al., 2009). The long-term average annual temperature at Gobabeb is 21.1°C (Lancaster et al., 1984) whereas the average annual precipitation is less than 100 mm (Eckardt et al., 2013) and highly variable (Peel et al., 2007). Consequently, the relatively frequent fog events are of special importance for the water balance of the Namib (Eckardt et al., 2013).

Figure 9 shows the mean fit errors (in-situ LST minus modelled LST) at 15 minutes interval for 54 days from Gobabeb, i.e. each data point represents the mean of 54 individual fit errors obtained at the corresponding solar time.

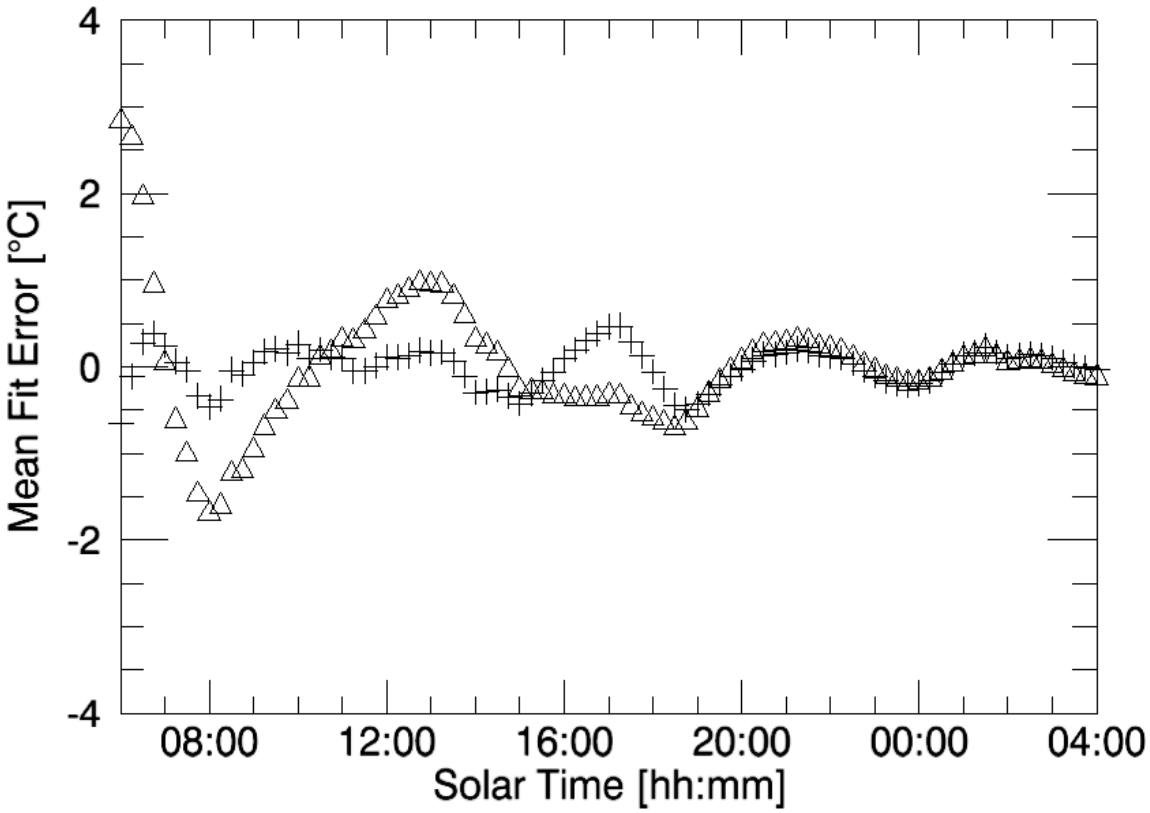

Figure 9 Crosses show the mean error at 15min interval over 54 days between LST derived from KT-15 East and Goe2009 LST at Gobabeb (05.12.2007 to 28.01.2008). Triangles show results for a previous version of the DTC model.

Figure 9 demonstrates the superior ability of the Goe2009 model to reproduce the DTC with considerably smaller values of mean fit error. However, in the late afternoon the mean fit error oscillates with amplitude of about 0.5°C, which suggests a relatively small, but systematic mismatch between model and measurements at this time of the day. At night time model errors are less than 0.5°C.

The histogram of daily mean absolute deviation of the Goe2009 model from measured LST is shown in Figure 10. The histogram represents the same 54 days used in Figure 9. The histogram mean is 0.62°C and only 2 days deviate by more than 1°C (Figure 10); bias is minimised by the fitting process and is practically zero. Furthermore, the histogram seems to indicate a bi-modal distribution with one peak near 0.5°C and a second one near 0.8°C: this could be interpreted as overlapping distributions for clear-sky DTC and for DTC with regular disturbances (e.g. wind).

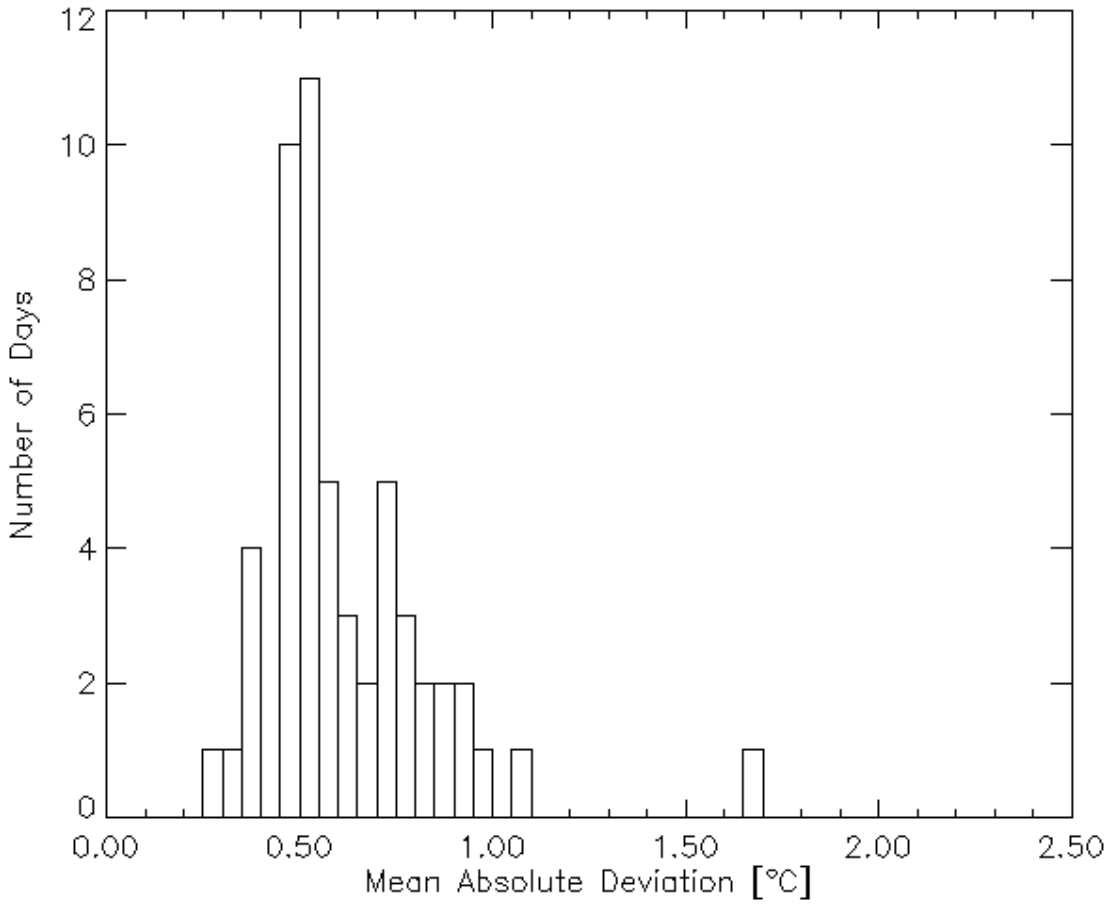

Figure 10 Histogram of mean absolute deviation per day for Goe2009 fitted to 54 diurnal temperature cycles measured at Gobabeb, Namibia.

4.3 Fits to decadal LST composites – The LSA-003B Product

Due to frequent cloud-cover continuous diurnal sequences of MLST (LSA-001) are usually not available. Therefore, LSA SAF's operational TSP product (LSA-003B) is generated from decadal LST composites (LSA-003A). Median and maximum composites form synthetic DTC reflecting the average ('most typical') LST and the highest LST for each MSG/SEVIRI time-slot during the compositing interval, respectively. TSP (LSA-003B) obtained for such decadal composites then provide a 10-day synthesis of up to 960 LSA SAF MLST files (LSA-001). Important quantities provided by the TSP are minimum temperature, maximum temperature and its time of occurrence, and the temperature decay constant (night-time cooling). For many applications the spatially smooth fields of modelled minimum temperature are of particular interest because satellite-retrieved LST tend to suffer from cloud-contamination (Göttsche and Olesen, 2009; Göttsche, 2014). Provided that the DTC model correctly describes a series of composite LST, the uncertainty of the modelled LST is lower than that of the composited LST, since the latter are based on a single or two MLST (LSA-001). Assuming a random scatter of composite LSTs around their true values, the simultaneous fitting of a series of LST composites will reduce uncertainty considerably, similar to averaging measurements. However, this improvement in uncertainty is difficult to quantify, since 'true' maximum and median LST at any given time are usually unknown: if suitable time series of in-situ LST are available, it may be quantified by comparing modelled in-situ LST composites with modelled satellite LST composites.

Figure 11 shows the mean absolute deviation between temperatures modelled with the determined TSP (LSA-003B) and the corresponding median LST (LSA-003A) for the period of the 11th to the 20th of June 2015. Low errors (light blue) correspond to areas with many cloud-free scenes during the compositing interval: this is where the sequence of LST composites approximates cloud-free DTC best.

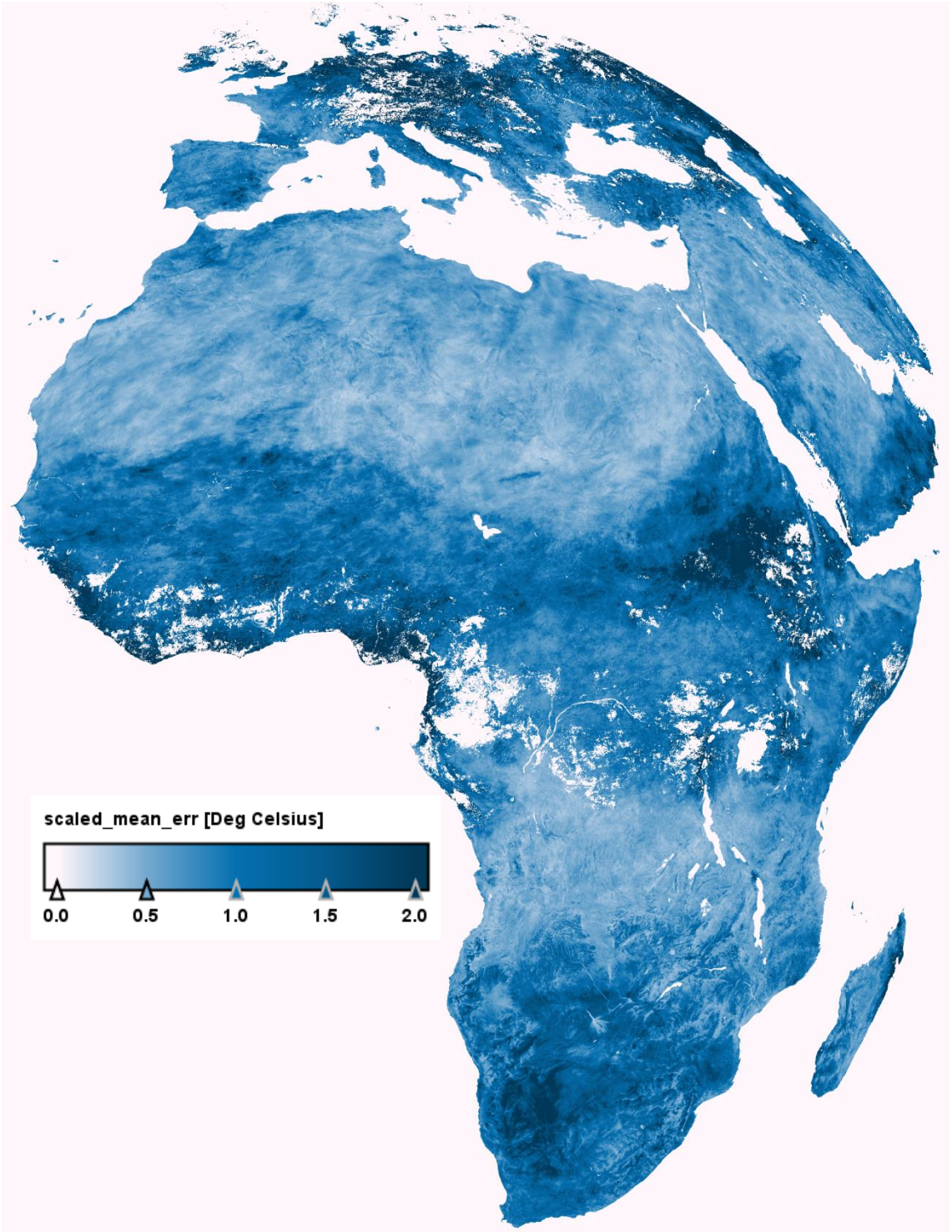

Figure 11 Mean error between modelled DTC and median LST (LSA-003A) obtained from the MLST (LSA-001) between the 11th and the 20th of June 2015. White: no data.

Figure 12 shows a subset of mean fit errors in Figure 11: the mean and the standard deviation within the blue rectangle are 0.73 K and 0.33 K, respectively. These values need to be compared to LSA

SAF's target accuracy of 2 K for the underlying MLST product and its accuracy of 1.0 K to 1.5 K when validated against in-situ measurements from Gobabeb, Namibia (Göttsche et al., 2013; Göttsche et al., 2016). Figure 13 shows a histogram for the errors within the blue rectangle: the bimodal distribution has a peak at about 0.5 K (upper half) and at 0.9 K (lower half). Based on these results it can be concluded that the Goe2009 model describes the DTC provided by sequences of temporal MLST composites (DLST; LSA-003A) well.

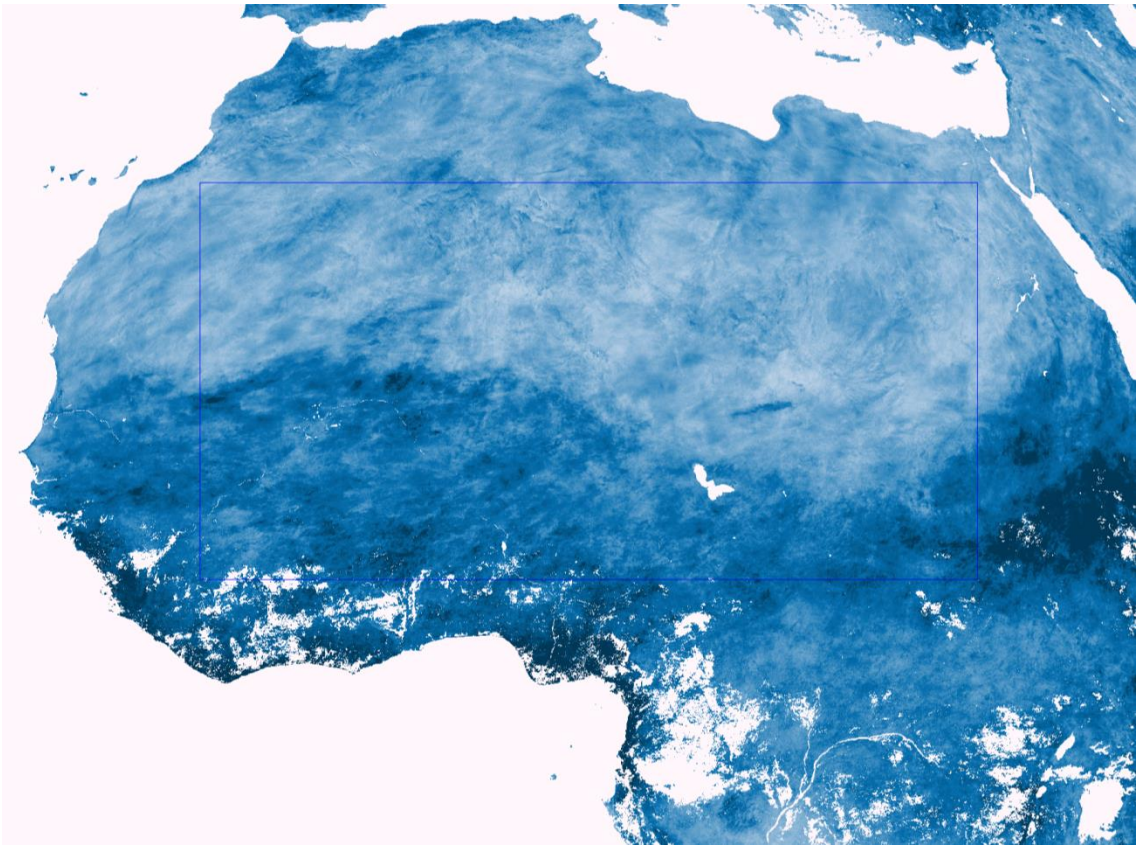

Figure 12 The blue rectangle marks the area used for obtaining the statistics (see text).

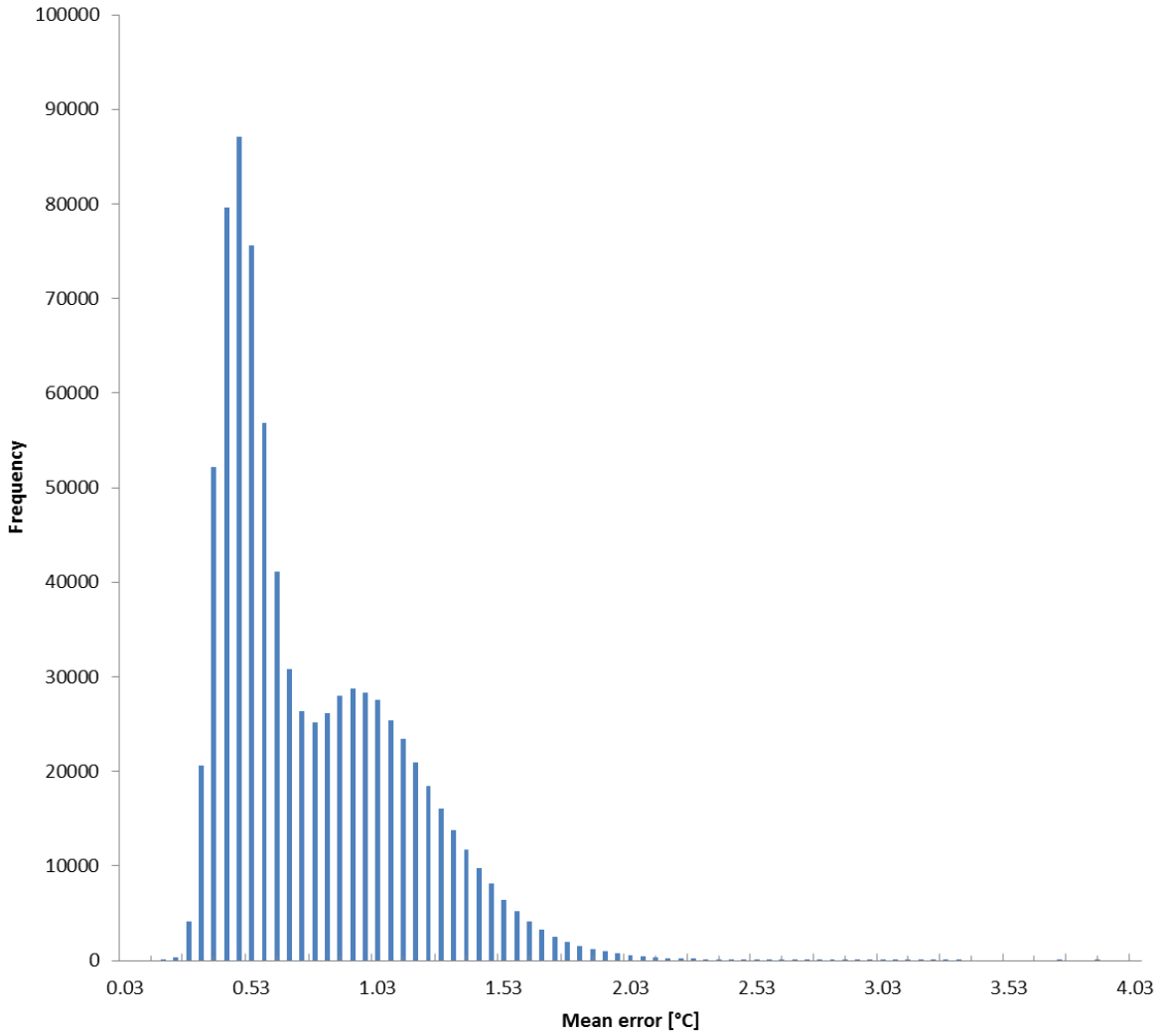

Figure 13 Histogram for the mean fit errors within the blue rectangle shown in Figure 12.

5 Concluding Remarks

The LSA-003A and LSA-003B products are derived from LSA SAF 15-min LST product estimated from SEVIRI/Meteosat (LSA-001). As such, the accuracy of LSA-003 largely depends on that of LSA-001 and on the correctness of the compositing algorithms applied. The LSA-001 product has been extensively validated against in situ stations (Ermida et al., 2014; Göttsche et al., 2016; Göttsche et al., 2013) and, for consistency assessment, also has been compared against other satellite products. The validation results for the input LSA-001 product are shown in the respective validation report (please see most recent version of SAF_LAND_VR_LST available at the LSA SAF site).

The correctness of the DLST median and maximum compositing algorithms (LSA-003A) was successfully tested with various combinations of synthetic LST input fields. Furthermore, analyses of composite products obtained for large parts of the MSG / SEVIRI earth disk were performed and satellite-derived composites were compared with composites of in-situ LST from validation station

Gobabeb, Namibia. The resulting differences in composite LST were within the range to be expected from the two different input data sets.

The Goe2009 model (Göttsche and Olesen, 2009), which is used in LSA-003B algorithm, was fitted to 54 DTC from a validation site in an arid climate (Gobabeb, Namibia) and to 100 DTC from a site in temperate climate (Evora, Portugal). The results demonstrate the high accuracy achieved by the DTC model with a limited set of parameters. The model was shown to describe the general shape of cloud-free DTC well: the average of daily mean absolute deviation between modelled and measured DTC is 0.62 °C for Gobabeb and 0.97 °C for Evora, where the latter is more effected by cloud-contamination. However, model performance strongly depends on the quality of the input LST as well as on atmospheric and surface wind conditions, i.e. the underlying DTC data should at least approximate an undisturbed DTC.

Generally, temporally continuous diurnal cycles of satellite-retrieved LST are not available. Therefore, the operational TSP product (LSA-003B) is generated from decadal LST composites (LSA-003A). The DLST product then provides a 10-day synthesis of the LSA SAF MLST product (LSA-001). For compositing periods with a sufficient number of cloud-free MLST (LSA-001), the mean absolute deviation between the sequence of LST composites and the modelled DTC is about half the MLST product's target accuracy. The effect of missing data was investigated by Göttsche and Olesen (2001) while a comparison of the Göttsche and Olesen models (2001 & 2009) with other models is given by Duan et al. (2012).

6 References

Duan, S.-B., Li, Z.-L., Wang, N., Wu, H., Tang, B.-H. (2012). Evaluation of six land-surface diurnal temperature cycle models using clear-sky in in situ and satellite data. *Remote Sensing of Environment*, 124, 15–25.

Eckardt, F.D., Soderberg, K.L., Coop, J., Muller, A.A., Vickery, K.J., Grandin, R.D., Jack, C., Kapalanga, T.S., and Henschel, J. (2013). The nature of moisture at Gobabeb, in the central Namib Desert. *Journal of Arid Environments*, 93, 7-19.

Ermida, S. L., I. F. Trigo, C. C. DaCamara, F. M. Göttsche, F. S. Olesen, G. Hulley (2014). Validation of remotely sensed surface temperature over an oakwood landscape – The problem of viewing and illumination geometries. *Remote Sensing of Environment*, 148, 16-27, doi: dx.doi.org/10.1016/j.rse.2014.03.016

Göttsche, F.-M., Olesen, F.-S., Trigo, I.F., Bork-Unkelbach, A., and Martin, M.A. (2016). Long term validation of land surface temperature retrieved from MSG/SEVIRI with continuous in-situ measurements in Africa. *Remote Sensing*, 8, 410, doi:10.3390/rs8050410.

Göttsche, F.-M. (2014). SAF for Land Surface Analysis (LSA SAF) Algorithm Theoretical Basis Document (ATBD) for Derived Products Land Surface Temperature (DLST), Prepared by the Land Surface Analysis Satellite Application Facility for EUMETSAT.

Göttsche, F.-M., Olesen, F.-S., and Bork-Unkelbach, A. (2013). Validation of land surface temperature derived from MSG/SEVIRI with in situ measurements at Gobabeb, Namibia. *International Journal of Remote Sensing*, 34(9-10), 3069-3083.

Göttsche, F.-M., and Olesen, F.S. (2009). Modelling the effect of optical thickness on diurnal cycles of land surface temperature. *Remote Sensing of Environment*, 113, 2306-2316.

Göttsche, F.-M., and Olesen, F.S. (2001). Modelling of diurnal cycles of brightness temperatures extracted from METEOSAT data. *Remote Sensing of Environment*, 76, 337-348.

Holben, B. N. (1986). Characteristics of maximum-value composite images from temporal AVHRR data. *International Journal of Remote Sensing*, 7, 1417–1734.

Hulley, G.C., Hook, S.J., Manning, E., Lee, S.-Y., and Fetzer, E. (2009). Validation of the Atmospheric Infrared Sounder (AIRS) version 5 land surface emissivity product over the Namib and Kalahari deserts. *Journal of Geophysical Research*, Vol. 114(D19).

Inamdar, A.K., French, A., Hook, S., and Vaughan, G. (2008). Land surface temperature retrieval at high spatial and temporal resolutions over the southwestern United States. *Journal of Geophysical Research*, 113, 1-18.

Inamdar, A.K., and French, A., (2009). Disaggregation of GOES land surface temperatures using surface emissivity. *Geophysical Research Letters*, 36(2), L02408.

Jiang, G.-M., Li, Z.-L., and Nerry, F. (2006). Land surface emissivity retrieval from combined mid-infrared and thermal infrared data of MSG-SEVIRI. *Remote Sensing of Environment*, 105, 326-340.

Köppen, W. (1936). Das geographische System der Klimate. *Handbuch der Klimatologie*. Gebr. Bornträger.

Lambin, E.F., and Ehrlich, D. (1996). The surface temperature-vegetation index space for land cover and land-cover change analysis. *Int. J. Remote Sens*., 17, 463-487.

Lancaster, J., Lancaster, N., and Seely, M.K. (1984). Climate of the central Namib Desert. *Madoqua*, Vol. 14(1), 5–61.

Peel, M.C., Finlayson, B.L., and McMahon, T. A. (2007). Updated world map of the Köppen-Geiger climate classification. *Hydrology and Earth System Sciences*, 11, 1633–1644.

Pereira, J.S., Mateus, J.A., Aires, L.M., Pita, G., Pio, C., David, J.S., Andrade, V., Banza, J., David, T.S., Paco, T.A., and Rodrigues, A. (2005). Net ecosystem carbon exchange in three contrasting Mediterranean ecosystems - the effect of drought. *Biogeosciences*, 4, 791–802.

Reuter, M. (2005). Identification of cloudy and clear sky areas in MSG SEVIRI images by analyzing spectral and temporal information. *Ph.D. Thesis* , Freie Universität Berlin

Schädlich, S., Göttsche, F.-M., and Olesen, F.-S. (2001). Influence of land surface parameters and atmosphere on METEOSAT brightness temperatures and interpolation of atmospheric correction. *Remote Sensing of Environment*, 75(1), 39-46.

Schmetz., J., Pili, P., Tjemkes, S., Just, D., Kerkman, J., Rota, S., and Ratier, A. (2002a). An introduction to Meteosat Second Generation (MSG). *Bull. Amer. Meteor. Soc.*, 83, 977-992.

Stöckli, R. (2013). The HelioMont Surface Solar Radiation Processing, *Scientific Report MeteoSwiss*, 93, ISSN: 1422-138, 122 pp.

Stoll, M.P. (1994). Potential of remote sensing in the thermal band for global change. In: Vaughan, R.A., & Cracknell, A.P. (Ed.), Remote sensing and global climate change, *NATO Advanced Science Institutes Series, Series I, 24* (pp. 393-404). Berlin: Springer Verlag

Trigo, I.F., Freitas, I. Monteiro, S. Coelho, F., Olesen, E. Kabsch, and F. Göttsche (2009a). SAF for Land Surface Analysis (LSA SAF) Validation Report LST, Prepared by the Land Surface Analysis Satellite Application Facility for EUMETSAT.